

Finite temperature crossovers near quantum tricritical points in metals

P. Jakubczyk,^{1,2,*} J. Bauer,² and W. Metzner²

¹*Institute for Theoretical Physics, Warsaw University, Hoża 69, 00-681 Warsaw, Poland*

²*Max-Planck-Institute for Solid State Research, Heisenbergstr. 1, D-70569 Stuttgart, Germany*

(Dated: May 23, 2022)

We present a renormalization group treatment of quantum tricriticality in metals. Applying a set of flow equations derived within the functional renormalization group framework we evaluate the correlation length in the quantum critical region of the phase diagram, extending into finite temperatures above the quantum critical or tricritical point. We calculate the finite temperature phase boundaries and analyze the crossover behavior when the system is tuned between quantum criticality and quantum tricriticality.

PACS numbers: 05.10.Cc, 73.43.Nq, 71.27.+a

I. INTRODUCTION

Quantum critical behavior in metals is a topic of prime interest for the theory and experiment in the field of condensed matter physics.¹⁻⁷ Despite significant effort made over the last couple of years, several intriguing puzzles remain unresolved by the quickly developing theory of quantum phase transitions. These include both, fundamental problems regarding the correct low energy action to describe quantum critical systems, and the physical mechanisms responsible for unusual behavior of specific compounds.

In the conventional scenario of quantum criticality the critical temperature T_c for a second order transition is driven to zero by a tuning parameter, so that a quantum critical point emerges. However, it is also possible that below a tricritical temperature the transition becomes first order. Then a particular brand of quantum criticality arises when the finite temperature (T) phase boundary terminates at $T = 0$ with the tricritical point. Strictly speaking, in real systems this scenario is hardly feasible, since it requires fine tuning of two non-thermal parameters. However, proximity to quantum tricriticality has been invoked to explain a number of experimentally observed properties of metallic compounds.⁸⁻¹³

Although the relevance of quantum tricriticality was emphasized in a number of recent works,¹⁰⁻¹³ a renormalization group (RG) study addressing crossovers between critical and tricritical behavior, in particular in the quantum-critical, non-Fermi liquid regime, is missing. In this paper we present a renormalization group analysis for a model system displaying such crossovers. We build upon an earlier work,¹⁴ where renormalization group flows of a quantum ϕ^6 -model were already studied. The main focus of that work was to show that order parameter fluctuations may turn first order transitions occurring within the bare model into continuous transitions.

The paper is structured as follows. In Sec. II we present a phenomenological picture of the problem to be analyzed, and in Sec. III we define the corresponding model action. In Sec. IV we describe the functional RG framework and derive the RG flow equations. In Sec. V we analyze the linearized forms of the flow equations obtaining analytical solutions in spatial dimensions $d > 2$. In Sec. VI we present example numerical results for the correlation length in the quantum critical regime, and the shapes of the phase boundaries. In the

final Sec. VII we lay out our conclusions.

II. PHENOMENOLOGICAL PICTURE

Before plunging into the details of the formalism let us consider the different scenarios which are envisaged in the following. In Fig. 1 (a) we schematically depict a generic phenomenological phase diagram of a system exhibiting a Gaussian quantum critical point (QCP). At $T = 0$ the system can be tuned between an ordered and a disordered state by varying a non-thermal control parameter r . At finite T , in the disordered phase, a crossover region, schematically represented here with a line, separates the Fermi liquid and quantum critical regimes. For $r < 0$, the T_c -line separates the phases of the system at finite T . The classical critical region where non-Gaussian fluctuations occur is bounded by the Ginzburg lines and vanishes as $T \rightarrow 0$.

By varying another system parameter the phase diagram can be continuously deformed so that the transition becomes first order at sufficiently low T , below a tricritical temperature T^{tri} (see Fig. 1 (c)). For a particular value of this parameter the tricritical point is located exactly at $T = 0$ so that the transition is second order for all $T > 0$ but the scaling properties of the system for $T \rightarrow 0$ are governed by the quantum tricritical point (QTCP) rather than the quantum critical point. This special scenario displaying a different scaling behavior is depicted in Fig. 1 (b). The purpose of the paper is to compute how the crossovers between the scenarios of Fig. 1 (a) through (b) to Fig. 1 (c) occur. Even in scenario (a) a “hidden” tricritical point, which would be present at $T^{\text{tri}} < 0$, i.e. the vicinity to a first order transition, can affect the scaling behavior at higher temperatures.

III. BARE ACTION

The conventional description of quantum criticality, which we shall rely upon here, invokes the Hertz action.¹⁵ This describes a bosonic mode overdamped by particle-hole excitations across the Fermi level and is applicable under the assumption that the electronic degrees of freedom may be integrated out. The original framework of Hertz¹⁵ and Millis¹⁶

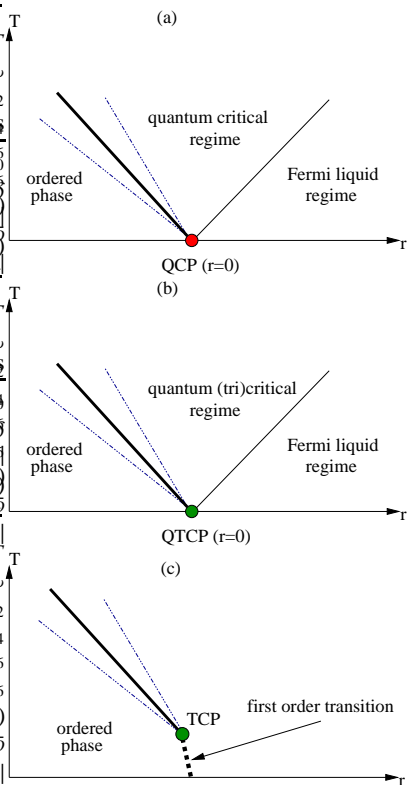


FIG. 1: (Color online) Different scenarios for generic phase diagrams. Bold solid (dotted) lines mark second (first) order phase transitions, thin solid lines indicate the crossover between quantum critical and Fermi liquid behavior, while the thin dotted lines indicate the boundaries of the Ginzburg region. (a) Schematic phase diagram of a system exhibiting a quantum critical point, at which a line of second order finite T phase transitions terminates. A crossover region, represented here with a line, separates the Fermi liquid and quantum critical regimes in the disordered phase. (b) Schematic phase diagram of a system exhibiting a quantum tricritical point. (c) Schematic phase diagram of a system exhibiting a tricritical point at a finite temperature. The transition is first order below the tricritical temperature. Critical quantum fluctuations are absent. Varying another control coupling one can tune between the depicted situations (see the main text).

was recently extended to account for a number of systems and phenomena not covered by the original studies. These include field-tuned quantum critical points,¹⁷ metamagnetic transitions,^{18,19} phase transitions induced by a non-equilibrium drive²⁰ as well as dimensional crossovers²¹ and quantum criticality involving multiple time scales.²² We focus on the case of discrete symmetry breaking, which can be described by a scalar order parameter field ϕ , and an action of the form

$$S[\phi] = \frac{T}{2} \sum_{\omega_n} \int \frac{d^d p}{(2\pi)^d} \phi_p \left(Z_\omega \frac{|\omega_n|}{|\mathbf{p}|^{z-2}} + Z\mathbf{p}^2 \right) \phi_{-p} + \mathcal{U}[\phi]. \quad (1)$$

Here ϕ_p with $p = (\mathbf{p}, \omega_n)$ is the momentum representation of the order parameter field, where $\omega_n = 2\pi nT$ with integer n denotes the (bosonic) Matsubara frequencies. Momentum and

energy units can be chosen such that the prefactors in front of $\frac{|\omega_n|}{|\mathbf{p}|^{z-2}}$ and \mathbf{p}^2 are equal to unity. The action is regularized in the ultraviolet by restricting momenta to $|\mathbf{p}| \leq \Lambda_0$. The term $\frac{|\omega_n|}{|\mathbf{p}|^{z-2}}$, where $z \geq 2$ is the dynamical exponent, effectively accounts for overdamping of the order-parameter fluctuations by fermionic excitations across the Fermi surface. The expression Eq. (1) is valid for $|\mathbf{p}|$, and $\frac{|\omega_n|}{|\mathbf{p}|^{z-2}}$ sufficiently small, which is the limit relevant for the physical situation considered.¹⁶

The quantity $\mathcal{U}[\phi]$ is a local effective potential which we expand to sixth order in ϕ :

$$\mathcal{U}[\phi] = \int_0^{1/T} d\tau \int d^d x U(\phi(x, \tau)), \quad (2)$$

where

$$U(\phi) = a_2 \phi^2 + a_4 \phi^4 + a_6 \phi^6. \quad (3)$$

This ansatz assumes the absence of a field explicitly breaking the inversion symmetry. We require $a_6 > 0$ to stabilize the system at large $|\phi|$. The bare effective potential yields the well known phase diagram,²³ exhibiting a second-order transition for $a_4 > 0$, a first order transition for $a_4 < 0$ and a tricritical point at $a_2 = a_4 = 0$. Within the present model the mass parameter a_2 plays the role of the non-thermal control parameter (r) to tune the transition. By varying the quartic coupling a_4 one can deform the phase diagram so that the transition is second or first order at low T (compare Fig. 1). In conventional quantum criticality, the temperature dependence of the coefficients a_2, a_4, a_6 can be neglected, as it leads only to subleading corrections. However, it turns out that in a quantum tricritical regime the generic quadratic temperature dependence of these coefficients yields a dominant contribution to the temperature dependence of the correlation length.

IV. FLOW EQUATIONS

In the present study we apply the one-particle irreducible variant of the functional RG.²⁴⁻²⁷ The derivation of the flow equations follows Ref. 14, where the present quantum ϕ^6 model was applied to analyze the effect of fluctuations on the order of quantum phase transitions and the shapes of the finite T phase boundaries. The starting point is the exact functional evolution equation²⁸

$$\frac{\partial}{\partial \Lambda} \Gamma^\Lambda[\phi] = \frac{1}{2} \text{Tr} \frac{\partial_\Lambda R^\Lambda}{\Gamma^{(2)}[\phi] + R^\Lambda} \quad (4)$$

describing the flow of the effective action $\Gamma^\Lambda[\phi]$, which is the generating functional for one-particle irreducible vertex functions as the infrared cutoff scale Λ is reduced. Here $\Gamma^{(2)}[\phi] = \delta^2 \Gamma^\Lambda[\phi] / \delta \phi^2$, $\text{Tr} = T \sum_{\omega_n} \int \frac{d^d p}{(2\pi)^d}$, finally R^Λ denotes the cutoff function added to the inverse propagator to cut off modes with momentum below the scale Λ . We implement the Litim cutoff²⁹

$$R^\Lambda(\mathbf{p}) = Z(\Lambda^2 - \mathbf{p}^2)\theta(\Lambda^2 - \mathbf{p}^2). \quad (5)$$

For $\Lambda = \Lambda_0$ the quantity Γ^Λ is just the bare action, while in the limit $\Lambda \rightarrow 0$ it converges to the full effective action, i.e., the Gibbs free energy. In most cases it is impossible to solve Eq. (4) in the full functional space. One may however cast it onto a suitably chosen set of flowing couplings. The approximation applied here amounts to assuming that the effective potential preserves the form given by Eq. (3) with flowing couplings, while the inverse propagator retains its initial form

$$\begin{aligned} G^{-1}(\mathbf{p}, \omega_n) &= \Gamma^{(2)}[\phi = \phi_0] + R^\Lambda(\mathbf{p}) \\ &= Z_\omega \frac{|\omega_n|}{|\mathbf{p}|^{\varepsilon-2}} + Z\mathbf{p}^2 + 2a_2 + R^\Lambda(\mathbf{p}), \end{aligned} \quad (6)$$

where ϕ_0 is the minimum of $U(\phi)$. The present study deals with situations where the quantum critical point is Gaussian. In the following we shall disregard the flow of Z , which is equivalent to neglecting the anomalous dimension of the order parameter field. Such a parameterization of the effective action does not capture the anomalous scaling behavior of the propagator in the narrow vicinity of the classical second-order phase transition at finite temperature. Analogous truncations retaining the flow of Z were applied in Refs. 14,30. The results of Ref. 30 indicate that universal aspects of the shape of the phase boundary are not affected by non-Gaussian thermal fluctuations. In the following we shall also neglect the renormalization of the factor Z_ω . The flow of Z_ω was computed in Ref. 30, and shown to be negligible. The present truncation reproduces the essential features of the system except for the narrow vicinity of the second order transition at $T > 0$, where nonetheless the shape of the phase boundary is described correctly. Note, however, that the approach can be adapted to capture the anomalous dimension of the order parameter field³⁰ and to deal with cases where the fixed point associated with the quantum critical point is not Gaussian.³¹ The present truncation is analogous to the zeroth order derivative expansion,^{24,25} which was applied extensively in the context of classical critical phenomena. The essential quantum ingredient present here is the Landau damping term $\frac{|\omega_n|}{|\mathbf{p}|^{\varepsilon-2}}$. On top of the derivative expansion we performed a polynomial expansion of the effective potential.

Relying on the truncation described above, the flow equation Eq. (4) can be reduced to a set of three ordinary differential equations which determine the flow of the couplings a_2, a_4, a_6 as functions of the cutoff scale Λ . In practice, whenever the effective potential features non-zero minima at $\pm\phi_0$, we find it more convenient to write the flow equations in terms of the variables $\rho_0 = \frac{1}{2}\phi_0^2, a_4, a_6$. The coupling a_2 is then obtained from

$$a_2 = -4\rho_0(a_4 + 3a_6\rho_0). \quad (7)$$

As long as there exists a non-zero ρ_0 , the evolution of the effective potential is given by the flow equations derived in Ref. 14,

$$\partial_t \rho_0 = 2v_d Z^{-1} \Lambda^{d-2} \left(3 + 2 \frac{6a_6\rho_0}{6a_6\rho_0 + a_4} \right) l_1^d, \quad (8)$$

$$\partial_t a_4 = 12v_d \Lambda^d \left[\frac{4}{3} l_2^d \frac{(30a_6\rho_0 + 3a_4)^2}{Z^2 \Lambda^4} - 5 l_1^d \frac{a_6}{Z \Lambda^2} \right] - 6\rho_0 \partial_t a_6, \quad (9)$$

$$\partial_t a_6 = 16v_d \Lambda^d \left[-\frac{8}{3} l_3^d \frac{(30a_6\rho_0 + 3a_4)^3}{Z^3 \Lambda^6} + 15 l_2^d a_6 \frac{30a_6\rho_0 + 3a_4}{Z^2 \Lambda^4} \right], \quad (10)$$

where $v_d^{-1} = 2^{d+1} \pi^{d/2} \Gamma(d/2)$ and $t = \log(\Lambda/\Lambda_0) \leq 0$. The threshold²⁴ functions $l_i^d(\delta)$ are determined from

$$l_i^d(\delta) = \frac{1}{4} v_d^{-1} \Lambda^{-d} \text{Tr} \frac{\partial_t R^\Lambda(\mathbf{p})}{Z_\omega \frac{|\omega_n|}{|\mathbf{p}|} + Z\mathbf{p}^2 + R^\Lambda(\mathbf{p}) + Z\Lambda^2 \delta}, \quad (11)$$

$$l_1^d(\delta) = -\frac{\partial}{\partial \delta} l_0^d(\delta), \quad (12)$$

$$l_n^d(\delta) = -\frac{1}{n-1} \frac{\partial}{\partial \delta} l_{n-1}^d(\delta), \quad n \geq 2. \quad (13)$$

In Eqs. (8, 9, 10) $\delta = \delta(\rho) = \frac{1}{Z\Lambda^2}(U'(\rho) + 2\rho U''(\rho))$ and the threshold functions are evaluated at the value of δ corresponding to ρ_0 , that is, $l_n^d = l_n^d(\delta)|_{\rho=\rho_0}$. The flow equations are illustrated in terms of Feynman diagrams in Fig. 2.

For $\rho_0 = 0$ the flow equations are simplified as the interaction vertices involving an odd number of legs (see Fig. 2) vanish. In terms of the couplings a_2, a_4, a_6 they yield

$$\partial_t a_2 = -24v_d \frac{a_4}{Z\Lambda^{2-d}} l_1^d, \quad (14)$$

$$\partial_t a_4 = v_d \Lambda^d \left[\left(12 \frac{a_4}{Z\Lambda^2} \right)^2 l_2^d - 60 \frac{a_6}{Z\Lambda^2} l_1^d \right], \quad (15)$$

$$\partial_t a_6 = v_d \Lambda^d \left[-\frac{2}{3} \left(12 \frac{a_4}{Z\Lambda^2} \right)^3 l_3^d + \left(12 \frac{a_4}{Z\Lambda^2} \right) \left(60 \frac{a_6}{Z\Lambda^2} \right) l_2^d \right]. \quad (16)$$

V. LINEARIZED FLOW EQUATIONS

Essential features of the solutions to the equations provided in the previous section (the values of the exponents describing the system in the quantum-critical regime in particular) can be computed analytically by taking only the dominant terms in the flow equations into account. Here we analyze the linearized version of the flow equations in spatial dimension $d > 2$. We shall use the following rescaled variables:

$$\delta = \frac{2a_2}{Z\Lambda^2}, \quad u = \frac{a_4}{Z^2 \Lambda^{4-d}}, \quad v = \frac{a_6}{Z^3 \Lambda^{6-2d}}. \quad (17)$$

We linearize the flow equations around the zero temperature Gaussian fixed point

$$\partial_t \delta = -2\delta - 48v_d l_1^d(\delta) u, \quad (18)$$

$$\partial_t u = (d-4)u - 60v_d l_1^d(\delta) v, \quad (19)$$

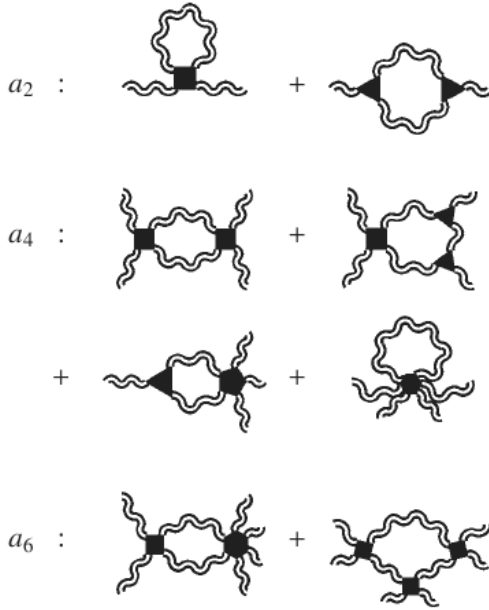


FIG. 2: Feynman diagrams representing the contributions to the flow equations for the couplings parameterizing the effective potential. Interactions involving an odd number of legs vanish if the system is in the disordered phase.

$$\partial_t v = (2d - 6)v. \quad (20)$$

All the resulting flow equations involve contributions from rescaling. In addition, renormalization of the couplings δ, u by the diagrams involving just one interaction vertex is retained. After this step, the terms involved are analogous to those analyzed by Millis,¹⁶ where $v = 0$, so that only mass renormalization from the tadpole diagram was considered. Note that in the present case of discrete symmetry-breaking, Eq. (18, 19, 20) are applicable both in the symmetric and symmetry-broken phases.

In the above form we still find the flow equations rather hard to solve by hand as the threshold function $l_1^d(\delta)$ involves integrals (see Eqs. (11,12)). Inspired by the seminal work by Millis,¹⁶ we additionally expand the function l_1^d for $\tilde{T} = \frac{2\pi T Z_\omega}{Z \Lambda^z} \ll 1$ and $\tilde{T} \gg 1$. In the regime $\tilde{T} \ll 1$ the flow is dominated by quantum physics, while for $\tilde{T} \gg 1$ the quantum contributions to the flow equations are negligible compared to the classical ones. Similarly to Ref. 16 we shall integrate the flow equations from $\Lambda = \Lambda_0$ to $\Lambda = \Lambda^*$ determined by $\tilde{T}(\Lambda^*) = 1$ using the equations valid strictly speaking for $\tilde{T} \ll 1$. The result will then serve as the initial condition for the solution of the flow from Λ^* to $\Lambda = 0$, where we shall in turn use the asymptotic flow equations valid in the classical sector $\tilde{T} \gg 1$.

Performing the abovementioned expansion of the threshold function l_1^d we find for $\tilde{T} \ll 1$

$$\partial_t \delta \approx -2\delta - 48v_d \frac{4T}{\tilde{T}} \frac{u}{d+z-2}, \quad (21)$$

$$\partial_t u \approx (d-4)u - 60v_d \frac{4T}{\tilde{T}} \frac{v}{d+z-2}; \quad (22)$$

while for $\tilde{T} \gg 1$

$$\partial_t \delta \approx -2\delta - 48v_d \frac{2T}{d} u, \quad (23)$$

$$\partial_t u = (d-4)u - 60v_d \frac{2T}{d} v. \quad (24)$$

The above equations, together with Eq. (20), form a set of linear ordinary differential equations of first order. Eq. (20) is solved immediately. Plugging the result into the flow of u and integrating, we calculate $u(\Lambda)$ for $\Lambda > \Lambda^*$ and $\Lambda < \Lambda^*$. Demanding that $a_4^r \equiv \lim_{\Lambda \rightarrow 0} a_4(\Lambda) = \lim_{\Lambda \rightarrow 0} Z^2 \Lambda^{4-d} u(\Lambda) > 0$ we find a condition for the occurrence of a second order transition. If $a_4^r(T) = 0$ at some $T \geq 0$, there is a tricritical point at this T . We find that the transition is always second order at sufficiently high T . It may turn first order as T approaches zero. The condition $a_4^r > 0$ yields

$$u_0 > -v_0 \left(C + C' T^{(d+z-2)/z} \right), \quad (25)$$

where $u_0 = u(\Lambda = \Lambda_0)$, $v_0 = v(\Lambda_0)$, and C, C' are positive constants (depending on $\Lambda_0, Z_\omega, Z, d$ and z). The explicit expressions for these constants are given in the Appendix. If the condition for u_0 given by Eq. (25) is fulfilled for $T = 0$, it clearly holds for any $T \geq 0$. In such case there is a line of critical points terminating at $T = 0$ with a QCP. This is the scenario (a) in Fig. 1. For $v_0 = 0$ one obviously recovers $u_0 > 0$ and the standard quantum critical behavior. A quantum tricritical point exists if $u_0 = u_0^{\text{tri}} = -Cv_0$, which corresponds to the quantum tricritical scenario (b) in Fig. 1. In case the condition Eq. (25) is violated at $T = 0$, it is still always fulfilled at sufficiently high temperatures, namely for $T > T^{\text{tri}}$, where

$$T^{\text{tri}} = [-(u_0/v_0 + C)/C']^{z/(d+z-2)}. \quad (26)$$

In this case the transition becomes first order for $T < T^{\text{tri}}$, which is scenario (c) in Fig. 1.

We now discuss the flow of δ . Plugging the solution obtained for $u(\Lambda)$ into Eq. (21, 23), we integrate Eq. (21) from Λ_0 to Λ^* . The solution at Λ^* is the initial condition for Eq. (23). In cases where critical behavior occurs, the correlation length can be extracted as $\xi^{-2} \propto \lim_{\Lambda \rightarrow 0} \Lambda^2 \delta$. The result has the following structure:

$$\xi^{-2} = D_0(T) + D_1 T^{(d+z-2)/z} + v_0 D_2 T^{(2(d+z)-4)/z}, \quad (27)$$

where D_0 depends on δ_0, u_0 and v_0 , while D_1 and D_2 do not depend on δ_0 . Notice that $D_1 = \bar{D}_1(u_0 - u_0^{\text{tri}})$, where $\bar{D}_1 > 0$. Explicit expressions are quoted in the Appendix. The generically quadratic temperature dependence of the bare model parameters δ_0, u_0 and v_0 for low T induces a corresponding quadratic temperature dependence of D_0, D_1, D_2 . While the temperature dependence of D_1 and D_2 is always negligible, the quadratic T -dependence of $D_0(T) = D_0 + D_0' T^2$ dominates in the tricritical regime (see below) and must therefore be kept.^{12,13}

Criticality occurs at $T = 0$ when $\delta_0 = \delta_0^{\text{cr}}$ such that $D_0 = 0$. At finite T the behavior of ξ^{-2} is governed by several terms. The quantum critical term $D_1 T^{(d+z-2)/z}$ dominates for sufficiently low T , provided $D_1 > 0$, and reproduces the result for $\xi^{-2}(T)$ derived already by Millis.¹⁶ Compared to that term, the quadratic temperature dependence from $D_0(T)$ and the term $v_0 D_2 T^{(2(d+z)-4)/z}$ coming from the ϕ^6 interaction are subleading corrections. On the other hand, if $u_0 = u_0^{\text{tri}}$, the coefficient D_1 becomes zero and the correlation length exhibits a different behavior,

$$\xi^{-2} = D'_0 T^2 + v_0 D_2 T^{(2(d+z)-4)/z}. \quad (28)$$

The exponent of the second term is 3 for $z = 2, d = 3$, and $8/3$ for $z = 3, d = 3$. The latter exponent was obtained already from a self-consistent fluctuation resummation.¹¹ At low temperatures the "trivial" quadratic term thus dominates the temperature dependence of ξ in the tricritical regime. The relevance of the quadratic temperature dependences of the bare parameters in the tricritical regime was noticed already by Misawa et al.^{12,13} However, the exponent for the temperature dependence of the order parameter susceptibility obtained by these authors for the quantum tricritical regime turned out to be identical to that for conventional quantum criticality, that is, $3/2$ for $z = 2$. That result, obtained from a self-consistent summation of staggered and homogeneous fluctuations, is clearly at variance with our result.³²

For quantum critical systems close to quantum tricriticality (small D_1), the correlation length follows a tricritical temperature dependence above a crossover temperature

$$T_{\text{cross}} = \left(\frac{D_1}{D'_0} \right)^{z/(2+z-d)}. \quad (29)$$

For the special case of a very small D'_0 , tricritical behavior with an exponent $\frac{2(d+z)-4}{z}$ is observed for temperatures above

$$T_{\text{cross}} = \left(\frac{D_1}{v_0 D_2} \right)^{z/(d+z-2)}. \quad (30)$$

Eq. (27) also yields the shape of the phase boundary. From the condition $\xi^{-2} = 0$ one finds $T_c \sim |\delta_0 - \delta_0^{\text{cr}}|^\psi$, where $\psi = \psi^{\text{qc}} = \frac{z}{d+z-2}$ for quantum criticality, reproducing the result by Millis.¹⁶ This value crosses over to $\psi = \psi^{\text{tri}} = \frac{1}{2}$ when the quartic coupling approaches the tricritical value u_0^{tri} . Only for the special case $D'_0 = 0$ one obtains $\psi^{\text{tri}} = \frac{z}{2(d+z)-4}$. For small $D'_0 \neq 0$ a crossover between different exponents occurs.

As already stated, for $u_0 < u_0^{\text{tri}}$ a classical tricritical point exists at $T = T^{\text{tri}} > 0$. In Eq. (27) this manifests itself by a negative value of D_1 . From the condition $\xi^{-2} = 0$ we find the shape of the phase boundary above $T = T^{\text{tri}}$ to follow $|\delta_0 - \delta_0^{\text{tri}}| \approx a|T - T^{\text{tri}}| + b|T - T^{\text{tri}}|^2$. This reproduces a MFT result for classical tricritical points.²³

From the solution for $\delta(\Lambda)$ we also read off the shape of the crossover line separating the Fermi liquid and the quantum critical regimes. The condition for the occurrence of the quantum disordered (Fermi liquid) regime¹⁶ is that the correlation length becomes of the order of the inverse upper cut-off before classical scaling is reached, that is, $\delta(\Lambda^*) > \Lambda^2$.

From this condition we find the shape of the crossover line as $\delta_0 - \delta_0^{\text{cr}} \sim T^{2/z}$, as can also be deduced by a phenomenological reasoning.^{1,2}

The linearized flow equations discussed above are not applicable in two dimensions. The reason is easily understood from the diagrammatic interpretation provided in Fig. 2. The tadpole diagram renormalizing the a_2 coefficient exhibits a logarithmic infrared singularity for $\xi \rightarrow \infty$ at $T > 0$. The divergence is cured when one accounts for the renormalization of the quartic interaction coupling via the terms of the order a_4^2 .

VI. NUMERICAL SOLUTIONS TO THE FLOW EQUATIONS

Here we present results from direct numerical solutions to the flow equations delivered in Sec. IV. Information concerning the physical state of the system is read off from the renormalized values of the quantities a_2, a_4, a_6 in the limit $\Lambda \rightarrow 0$, $a_n^r = \lim_{\Lambda \rightarrow 0} a_n(\Lambda)$. In all numerical computations we put $Z = 1, Z_\omega = 1, \Lambda_0 = 1$ and $a_6^0 = a_6(\Lambda_0) = 1$. We omit the quadratic T -dependence of a_2 in this section. We analyze solutions to the flow equations upon varying the parameters $a_2^0 = a_2(\Lambda_0), a_4^0 = a_4(\Lambda_0)$ and T . We refer to Ref. 14 for example plots of the numerically computed phase boundaries including cases involving a first order transition. Here we focus on the situation where a_4^0 is close to a $a_4^{0,\text{tri}}$, a value where a tricritical point exists at $T = 0$ for some a_2^0 . In the analytical calculation based on the linearized equations one finds the quantum tricritical point for the choice $a_4^0 = a_4^{0,\text{tri}} = -\frac{120\Lambda_0^{d+z-2}v_d}{\pi(d+z-2)^2}a_6^0$. For $d = z = 3, \Lambda_0 = a_6^0 = 1$ this gives $a_4^{0,\text{tri}} \approx -0.0302358$. In the numerical solution for the full flow equations a value for $a_4^{0,\text{tri}}$ emerges on fine tuning a_2^0 and a_4^0 , such that $a_2^r \approx a_4^r \approx 0$, where the value for a_4^0 tends to come out a bit (by less than 1%) smaller than the analytical estimate.

Once the transition line is established, we can fix a_4^0 and investigate the quantum critical regime spanning over the quantum critical or tricritical point. In particular, we extract the correlation length ξ as function of T . In the region of interest the system is typically ordered within the bare model ($a_4^0 < 0, a_2^0 > 0$, but $(a_4^0)^2 > 4a_2^0 a_6^0$), but becomes disordered in the course of the flow, as the order parameter becomes zero for some finite Λ . At this scale we have to switch to the set of equations valid in the symmetric phase (see Sec. IV).

We first show results for pure tricritical scaling of the inverse correlation length ξ^{-2} as a function of temperature (see Fig. 3). We set $d = z = 3$ and we choose the parameter $a_4^0 \approx a_4^{0,\text{tri}}$ and a_2^0 tuned to the zero temperature quantum tricritical point. This corresponds to the situation depicted in Fig. 1 (b), where the QTCP is approached from above. Over a wide range of temperature we find that the slope $\epsilon = 2.66$ gives a good fit to the numerical data, corresponding to the analytically derived value $1/\psi^{\text{tri}} = 8/3$. The leveling off at low temperatures could be avoided by further fine-tuning a_4^0 , while for higher temperature the slope decreases as non-universal features start to play a role towards the cut-off scale.

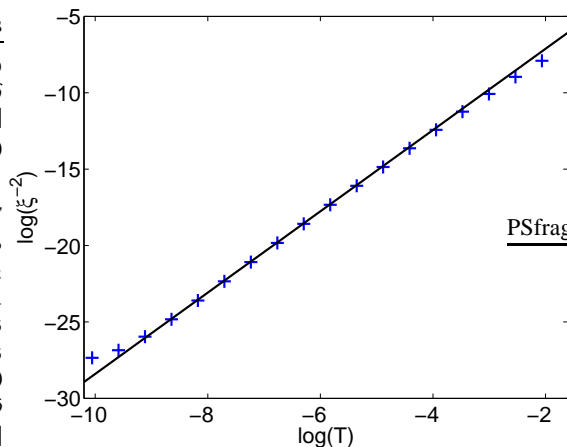


FIG. 3: (Color online) The logarithm of the inverse correlation length ξ^{-2} versus $\log(T)$ in the quantum tricritical regime in $d = z = 3$. The special choice of parameters is $a_4^0 = -0.030270317439$ and $a_2^0 = 0.00018421858$.

If the value of a_4^0 is increased slightly above $a_4^{0,\text{tri}}$ and a_2^0 again tuned to the zero temperature quantum critical point the crossover behavior in the correlation length as derived in equation (27) appears. Results of the numerical computations demonstrating this crossover behavior of the correlation length are displayed in Fig. 4.

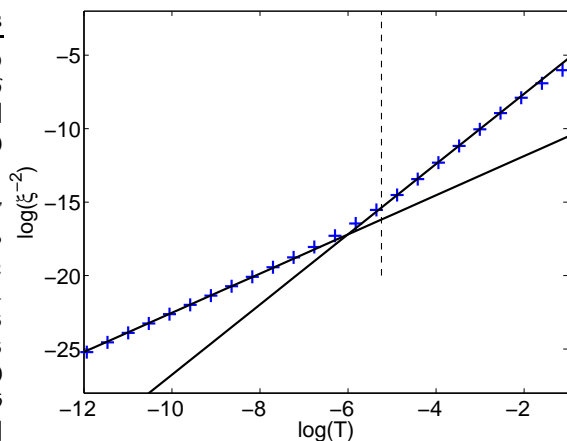


FIG. 4: (Color online) Correlation length versus temperature in the quantum critical regime in $d = z = 3$. The plot parameters are $a_4^0 = -0.03$ slightly above the tricritical value and $a_2^0 = 0.0001809109296$ tuned to the zero temperature transition point. The vertical dashed line gives the analytical crossover temperature as obtained from Eq. (30). The fits (straight lines) are discussed in the text.

At low temperature the slope $\epsilon = 1.33$ fits well to the quantum critical scaling $1/\psi_{\text{qc}} = 4/3$. For larger temperatures the fit gives $\epsilon = 2.39$, which lies about 10% below the value expected $1/\psi^{\text{tri}}$. This can be explained with deviations from the power law at higher energy as noted in the discussion of Fig. 3. On choosing a value of a_4^0 closer to the tricritical one

the crossover temperature decreases. The (low T) region characterized by the standard quantum critical scaling shrinks and tricritical scaling down to $T = 0$ sets in, which is accompanied by ϵ approaching the value $8/3$ (see Fig. 3).

We now turn to the phase boundary. The result computed for the quartic coupling a_4^0 fine-tuned to its tricritical value is exhibited in Fig. 5. The shape of the phase boundary follows

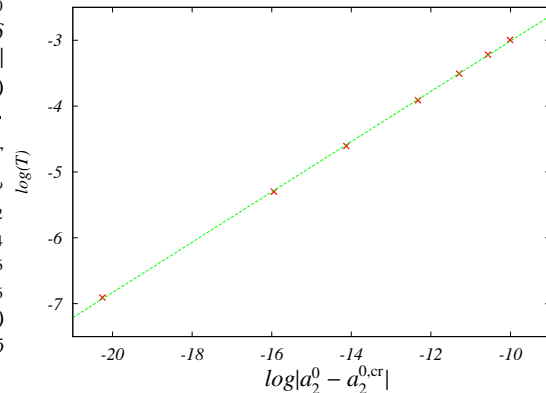


FIG. 5: (Color online) Transition line in $d = z = 3$. The quartic coupling is chosen close to the tricritical value $a_4^0 = -0.03027 \approx a_4^{0,\text{tri}}$.

the power law $T \sim |a_2^0 - a_2^{0,\text{cr}}|^\psi$. In the double logarithmic plot we find the slope $\epsilon \approx 0.378$, which compares well to the value $\psi^{\text{tri}} = 3/8$ obtained analytically in Sec. V. When the quartic coupling is increased, the system shows the Hertz-Millis scaling with $\psi^{\text{qc}} = 3/4$ for low temperature, and at larger temperature tricritical scaling with $\psi^{\text{tri}} = 3/8$ is still visible for the right choice of parameters (compare Ref. 14).

VII. SUMMARY

We have presented a study of crossover behavior occurring in the vicinity of metallic quantum critical and tricritical points. The analysis is based on renormalization group flow equations derived within the functional RG framework applied to the Hertz action, retaining a ϕ^6 term. It complements and extends an earlier work (Ref. 14), providing results in the quantum critical regime and delivering analytical insights. We focused on crossovers occurring in the temperature dependence of the correlation length and the shape of the phase boundary in the quantum critical regime above the quantum critical and tricritical points in the phase diagram. The linearized form of the flow equations could be solved analytically in $d > 2$, yielding exponents for the power-laws obeyed by the correlation length and phase boundary. The analytical solutions were confirmed and complemented by a numerical evaluation of the full integro-differential flow equations. In the quantum tricritical regime the power-law contribution to the inverse correlation length generated by the ϕ^6 interaction provides only a subleading correction to the generic quadratic temperature dependence induced by the temperature

dependence of the coefficients in the bare action. For quantum critical systems close to quantum tricriticality, we computed the crossover temperature above which tricritical scaling is observed. In the situation where a tricritical point occurs at $T > 0$, we obtained an expression for the tricritical temperature, and recovered the shift exponent corresponding to the classical theory of tricriticality.

Acknowledgments

The authors would like to thank M. Nieszporski, S. Takei, H. Yamase for valuable discussions, and S. Takei for a careful reading of the manuscript. PJ was partially supported by the German Science Foundation through the research group FOR 723.

Appendix A: Explicit expressions for the constants in Section V

In this Appendix we give explicit expressions for the constants appearing in the solutions to the flow equations in Sec. V. For the equations for $u(\Lambda)$ we have introduced

$$C = A\Lambda_0^z, \quad (\text{A1})$$

and

$$C' = \Lambda_0^{2-d} \left(\frac{2\pi Z\omega}{Z} \right)^{\frac{d-2}{z}} \left(B - \frac{2\pi Z\omega}{Z} A \right). \quad (\text{A2})$$

For $\delta(\Lambda)$ one has

$$D_0 = \delta_0 \Lambda_0^2 + A' \left(u_0 + \frac{1}{2} v_0 A \Lambda_0^z \right) \Lambda_0^{z+2}, \quad (\text{A3})$$

and

$$D_1 = \Lambda_0^{4-d} \left(u_0 + v_0 A \Lambda_0^z \right) \left(\frac{2\pi Z\omega}{Z} \right)^{\frac{d-2}{z}} \times \left[B' - A' \left(\frac{2\pi Z\omega}{Z} \right) \right],$$

and

$$D_2 = \frac{A' A \Lambda_0^{6-2d}}{2} \left(\frac{2\pi Z\omega}{Z} \right)^{\frac{2(d+z)-4}{z}} + \left[B' \Lambda_0^{6-2d} \left[\frac{B}{2} \left(\frac{2\pi Z\omega}{Z} \right)^{\frac{2d-4}{z}} - A \left(\frac{2\pi Z\omega}{Z} \right)^{\frac{2d+z-4}{z}} \right] \right],$$

where

$$A = 120v_d \frac{Z}{\pi Z\omega} \frac{1}{(d+z-2)^2}, \quad (\text{A4})$$

$A' = 96A/120$ and

$$B = \frac{120v_d}{d(d-2)}, \quad B' = \frac{96v_d}{d(d-2)}. \quad (\text{A5})$$

* Electronic address: Pawel.Jakubczyk@fuw.edu.pl

- ¹ S. Sachdev, *Quantum Phase Transitions* (Cambridge University Press, Cambridge, U.K., 1999).
- ² M. Vojta, Rep. Prog. Phys. **66** 2069 (2003).
- ³ H. v. Löhneysen, A. Rosch, M. Vojta, and P. Wölfle, Rev. Mod. Phys. **79**, 1015 (2007).
- ⁴ D. Belitz, T.R. Kirkpatrick, and T. Vojta, Rev. Mod. Phys. **77**, 579 (2005).
- ⁵ A. Abanov, A. V. Chubukov, and J. Schmalian, Adv. Phys. **52**, 119 (2003).
- ⁶ P. Gegenwart, Q. Si, and F. Steglich, Nature Phys. **4**, 186 (2008).
- ⁷ G. R. Stewart, Rev. Mod. Phys. **73**, 797 (2001).
- ⁸ C. Pfleiderer, S. R. Julian, and G. G. Lonzarich, Nature **414**, 427 (2001).
- ⁹ M. Uhlarz, C. Pfleiderer, and S. M. Hayden, Phys. Rev. Lett. **93**, 256404 (2004).
- ¹⁰ D. Belitz, T. R. Kirkpatrick, and J. Rollbuhler, Phys. Rev. Lett. **94**, 247205 (2005).
- ¹¹ A. G. Green et al. Phys. Rev. Lett. **95**, 086402 (2005).
- ¹² T. Misawa, Y. Yamaji, and M. Imada, J. Phys. Soc. Jpn. **77**, 093712 (2008).
- ¹³ T. Misawa, Y. Yamaji, and M. Imada, J. Phys. Soc. Jpn. **78**, 084707 (2009).
- ¹⁴ P. Jakubczyk, Phys. Rev. B **79**, 125115 (2009).
- ¹⁵ J.A. Hertz, Phys. Rev. B **14**, 1165 (1976).
- ¹⁶ A.J. Millis, Phys. Rev. B **48**, 7183 (1993).
- ¹⁷ I. Fischer, A. Rosch, Phys. Rev. B **71**, 184429 (2005).
- ¹⁸ A. J. Millis, A. J. Schofield, G. G. Lonzarich, and S. A. Grigera, Phys. Rev. Lett. **88**, 217204 (2002).

- ¹⁹ A. J. Schofield, A. J. Millis, S. A. Grigera, and G. G. Lonzarich, in *Ruthenate and rutheno-cuprate materials: unconventional superconductivity, magnetism, and quantum phase transitions*, edited by C. Noce, (Springer, Berlin, 2002).
- ²⁰ A. Mitra, S. Takei, Y. B. Kim, and A. J. Millis, Phys. Rev. Lett. **97**, 236808 (2006).
- ²¹ M. Garst, L. Fritz, A. Rosch, M. Vojta, Phys. Rev. B **78**, 235118 (2008).
- ²² M. Zacharias, P. Woelfle, M. Garst, Phys. Rev. B **80**, 165116 (2009); S. Takei, W. Witczak-Krempa, and Y. B. Kim, arXiv:0911.1133v1.
- ²³ I. D. Lawrie and S. Sarbach in *Phase Transitions and Critical Phenomena vol 9* ed. by C. Domb and J. L. Lebowitz (Academic Press, London 1984).
- ²⁴ J. Berges, N. Tetradis, and C. Wetterich, Phys. Rep. **363**, 223 (2002).
- ²⁵ B. Delamotte, D. Mouhanna and M. Tissier, Phys. Rev. B **69** 134413 (2004); B. Delamotte, arXiv:cond-mat/0702365 (2007).
- ²⁶ J. Pawłowski, Ann. Phys. **322**, 2831 (2007).
- ²⁷ H. Gies, arXiv:hep-ph/0611146 (unpublished).
- ²⁸ C. Wetterich, Phys. Lett. B **301**, 90 (1993).
- ²⁹ D.F. Litim, Phys. Rev. D **64**, 105007 (2001).
- ³⁰ P. Jakubczyk, P. Strack, A. A. Katanin, and W. Metzner, Phys. Rev. B **77**, 195120 (2008).
- ³¹ P. Strack and P. Jakubczyk, Phys. Rev. B **80**, 085108 (2009).
- ³² Note that in the absence of an anomalous dimension the order parameter susceptibility and ξ^2 obey the same power-law.